Nonmonotonic T_C Trends in Bi-Based Ferroelectric Perovskite Solid Solutions

Ilya Grinberg and Andrew M. Rappe

The Makineni Theoretical Laboratories, Department of Chemistry, University of Pennsylvania, Philadelphia, Pennsylvania 19104-6323, USA

(Received 28 July 2006; published 19 January 2007)

We use first-principles density functional theory calculations to investigate the strongly nonlinear compositional trends in ferroelectric $BiBO_3$-$PbTiO_3$ solid solutions for a variety of cations on the perovskite B site. We demonstrate that previously tabulated crystal chemical parameters (extracted from other Pb-based perovskite alloys [Grinberg *et al.*, J. Appl. Phys. **98**, 094111 (2005)]) permit accurate prediction of cation displacements in these new Bi-Pb alloys. We find that observed transition temperatures in these materials are well correlated with computed polarization magnitudes. The presented model for coupling between compositional variation and cation displacements explains the highly nonlinear and often nonmonotonic dependence of the Curie temperature (T_C) on composition observed in these solid solutions.

DOI: 10.1103/PhysRevLett.98.037603 PACS numbers: 77.80.−e, 71.15.Mb, 77.84.Dy, 78.20.Bh

Prediction of material properties from composition is a fundamental goal of materials science and a vital requirement for effective computational materials design. Despite intense theoretical and experimental research [1–8], this capability has only been partially achieved for the technologically important ferroelectric and piezoelectric perovskite solid solutions.

Recently, Bi perovskite alloys with $PbTiO_3$ (PT) have been shown to be promising candidates for new, lead-free or lead-reduced piezoelectrics with improved properties [9–14]. These studies have also revealed an important and unexpected difference between the classic Pb-based ferroelectric solutions and the new Bi-containing materials. Contrary to the linear dependence on composition mostly observed for Pb-based systems, ferroelectric to paraelectric transition temperatures of all $BiBO_3$-PT solid solutions exhibit strongly nonlinear and often nonmonotonic dependence of T_C and c/a on composition. For some cases, $BiBO_3$ substitution results in continuously increasing or decreasing T_C and c/a [11,12]. In others, T_C and c/a show an increase for small $BiBO_3$ fraction (x) and then decrease [11,13,14]. These observations are completely inconsistent with the intuitive expectation that the alloy's properties should be a mixture of the two end-members. The microscopic mechanisms behind these effects are currently poorly understood [15,16], hindering the search for new materials with enhanced properties.

Here, by analyzing a variety of $BiB^{2+}_{1/2}B^{4+}_{1/2}O_3$-PT alloys with first-principles calculations, we show that their anomalous compositional trends can all be explained using simple crystal chemical properties of the constituent atoms augmented by a surprisingly strong coupling between A cations and B cations.

To understand the relationships between atomic properties and overall structure, we study a series of $BiB^{2+}B^{4+}O_3$-PT (B^{2+} = Mg, Zn; B^{4+} = Zr, Ti) solid solutions, which span the range of behaviors observed in $BiBO_3$-PT systems [Fig. 1(a)]. The $BiZn_{1/2}Ti_{1/2}O_3$-PT (BZT-PT) solid solution exhibits a positive curvature parabolic dependence of T_C on x, with T_C reaching 1000 K at $x = 0.4$, the limit of BZT solubility in PT. This is currently the highest T_C observed for any PT solid solution. On the other hand, $BiMg_{1/2}Zr_{1/2}O_3$-PT (BMZ-PT), $BiMg_{1/2}Ti_{1/2}O_3$-PT (BMT-PT) and $BiZn_{1/2}Zr_{1/2}O_3$-PT (BZZ-PT) solid solutions show negative curvature parabolic dependence of T_C on x. In the case of BMZ-PT, the initial rise in T_C is essentially negligible, while for BMT-PT and BZZ-PT it is more significant. For BMZ-PT, T_C decreases rapidly, and at 50:50 composition it is $\approx$ 300 K lower than the T_C of PT. BZZ-PT exhibits a nonmonotonic dependence, with an initial rise and a drop in T_C for $x > 0.15$. A similar nonmonotonic trend is observed for BMT-PT as well, but with a much smaller curvature, with T_C varying by less than 30 K from $x = 0$ to $x = 0.5$.

First-principles plane-wave pseudopotential [17–19] density functional theory (DFT) [20,21] calculations were performed using $2 \times 2 \times 2$ 40-atom supercells with periodic boundary conditions at experimental volume [11,12]. For the BZZ-PT 50:50 composition, no experimental data are available (due to low solubility of BZZ in PT), so the lattice parameters were extrapolated from BZZ-PT compositions with lower BZZ content. The computational approach is the same as in previous work [22]. We use five different cation arrangements with minimal oxygen over- and underbonding [22–24] to study $x = 0.25$ and $x = 0.5$ compositions. Data for BZT-PT are taken from our previous study [25]. The polarization [26] and structural data obtained from DFT calculations are presented in Tables I and II.

In our examination of the composition-structure relationships in the $BiBO_3$-PT family, we focus on the displacement magnitude D_M of a cation from its ideal perovskite position. In an ideal perovskite, the center of the oxygen cage and the metal ion are located at the same point and polarization is therefore zero. In the actual, lower-symmetry structure, the displacements of the metal

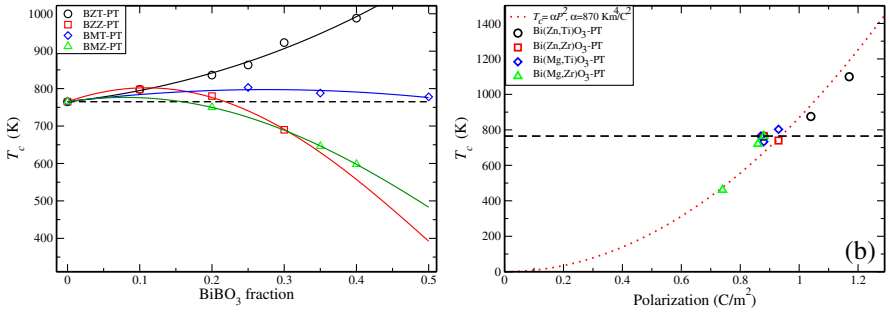

FIG. 1 (color online). (a) Experimental variation in T_C for BZT-PT, BZZ-PT, BMT-PT, and BMZ-PT solid solutions. Experimental data points shown by symbols. T_C of PT shown by dashed line. (b) Correlation between theoretical P values and experimentally observed T_C values. The dotted line shows a fit of experimental T_C data to theoretical P data, using $T_C = \alpha P^2$.

ions (with Born effective charge Z^*) away from the center of the oxygen cages generate local polarization and give rise to ferroelectricity.

From a comparison of the P and T_C data [Table I, Fig. 1(b)] it is clear that relation $T_C = \alpha P^2$ derived from Landau theory [22,28] quantitatively relates theoretical polarizations and experimental T_C values for $BiB^{2+}_{1/2}B^{4+}_{1/2}O_3$-PT systems. This relationship between P and T_C links changes in local equilibrium structure to changes in collective response at finite temperature. Thus, understanding how $BiB'B''O_3$ substitution affects material polarization is a key to explaining the compositional dependence of ferroelectric T_C.

Changes in P are mainly the result of changes in cation displacements D_M, since Z^* values are fairly transferable among ferroelectric perovskites [29]. Examination of Table II shows that displacement magnitudes for all cations depend on composition in a systematic way. Displacements are the largest for compositions with high concentration of Zn and Ti ions and are the smallest for Mg- and Zr-rich systems. This means that A-site and B-site displacements are strongly coupled [4,30]. Such systematic variation also means that D_M values can be predicted from the average crystal chemical characteristics of the solid solution A- and B-sites. Ionic size has long been used to explain properties in perovskites [9,31]. We have shown that displacement magnitudes of B cations in their O_6 cages are also transferable among $PbTiO_3$ solid solutions [27].

To identify and understand cation displacements in complex alloys, we create a model for ferroelectric displacement coupling. We claim that D_M, the displacement magnitude (averaged over all the M ions in the alloy) for a particular cation species M, varies in a range around a reference value for that cation, D^0_M, as the alloy composition is changed. Based on calculations in this and previous [10,27] work, we have established reference displacement magnitudes (D^0_M) for each cation (Table III), that each cation species would make in nearly pure $PbTiO_3$. The

TABLE I. Comparison of DFT polarization (P) calculations and experimental T_C results [11,12]. From the scatter in P values among the DFT supercells, we estimate the error in P values to be ± 0.02 C/m^2 and ± 0.06 C/m^2 for $x = 0.25$ and $x = 0.50$ compositions, respectively. T signifies experimentally tetragonal system, and R marks compositions experimentally found to be rhombohedral. P values are in C/m^2, T_C in K. Polarization magnitudes along the (100) direction are presented for all tetragonal compositions. For the rhombohedral BMZ-PT 50:50 system, P magnitude along the (111) direction is shown.

	Phase	P_{avg}	T_C
PT	T	0.87	765
25:75 BZT-PT	T	1.04	875
50:50 BZT-PT	T	1.17	1100
25:75 BZZ-PT	T	0.93	740
50:50 BZZ-PT	T	0.83	
25:75 BMT-PT	T	0.93	803
50:50 BMT-PT	T	0.88	733
25:75 BMZ-PT	T	0.86	721
50:50 BMZ-PT	R	0.74	461

TABLE II. Structural data for A- and B-site cations obtained from analysis of relaxed DFT $BiBO_3$-PT structures. Ground-state cation displacements from center of oxygen cages in Å. The first set of data is for total local displacement magnitudes. The second set is for the (100) component of displacements. $\bar{D}^0_B$ are obtained from Eq. (1) using D^0_B values taken from Ref. [27].

	D_{Bi}	D_{Pb}	$D_{B'}$	$D_{B''}$	D_{Ti}	$\bar{D}^0_B$
PT		0.45			0.28	0.250
25:75 BZT-PT	0.82	0.49	0.38	0.32	0.32	0.250
50:50 BZT-PT	0.90	0.56	0.50	0.34	0.34	0.250
25:75 BZZ-PT	0.79	0.47	0.34	0.21	0.27	0.235
50:50 BZZ-PT	0.84	0.48	0.48	0.20	0.19	0.220
25:75 BMT-PT	0.80	0.44	0.17	0.27	0.27	0.230
50:50 BMT-PT	0.77	0.42	0.20	0.26	0.26	0.208
25:75 BMZ-PT	0.79	0.42	0.20	0.17	0.25	0.214
50:50 BMZ-PT	0.77	0.39	0.16	0.14	0.21	0.178
PT		0.45			0.28	0.250
25:75 BZT-PT	0.79	0.47	0.38	0.31	0.31	0.250
50:50 BZT-PT	0.81	0.54	0.50	0.36	0.32	0.250
25:75 BZZ-PT	0.74	0.43	0.34	0.20	0.26	0.235
50:50 BZZ-PT	0.66	0.42	0.36	0.16	0.19	0.220
25:75 BMT-PT	0.76	0.42	0.17	0.27	0.27	0.230
50:50 BMT-PT	0.66	0.37	0.20	0.20	0.20	0.208
25:75 BMZ-PT	0.74	0.39	0.18	0.17	0.23	0.214
50:50 BMZ-PT	0.62	0.30	0.12	0.04	0.15	0.178

TABLE III. Reference displacement values D_M^0 [27] and coupling constants a_M and b_M for x-component and total cation displacement magnitudes. D_M^0 in Angstroms, a_M and b_M are dimensionless.

	D_M^0	$a_{M(\mathrm{tot})}$	$b_{M(\mathrm{tot})}$	$a_{M(x\mathrm{dir})}$	$b_{M(x\mathrm{dir})}$
Bi	0.80	1.03	2.50	0.23	2.73
Pb	0.45	0.51	2.33	0.57	3.22
Ti	0.25	0.34	1.74	0.11	2.46
Zr	0.13	−0.23	1.50	−0.23	2.50
Mg	0.08	0.46	1.27	0.69	2.30
Zn	0.25	1.56	1.03	1.14	4.24

deviation $\Delta D_M \equiv D_M - D_M^0$ from the reference displacement will be linearly proportional to ferroelectric environment changes away from that of $PbTiO_3$.

We describe the environment that the cations experience in a $BiB^{2+}_{1/2}B^{4+}_{1/2}O_3$-PT alloy with site-averaged reference displacement magnitudes:

$$\bar{D}_A^0 \equiv xD_{\mathrm{Bi}}^0 + (1-x)D_{\mathrm{Pb}}^0$$
$$\bar{D}_B^0 \equiv \frac{x}{2}(D_{\mathrm{B}^{2+}}^0 + D_{\mathrm{B}^{4+}}^0) + (1-x)D_{\mathrm{Ti}}^0. \quad (1)$$

To quantify changes in environments, we define the reference displacement change ΔD_A^0 and ΔD_B^0 as one Pb or Ti ion is replaced by the A or B cations of the dopant:

$$\Delta D_A^0 \equiv D_{\mathrm{Bi}}^0 - D_{\mathrm{Pb}}^0, \qquad \Delta D_B^0 \equiv \frac{1}{2}D_{\mathrm{B}^{2+}}^0 + \frac{1}{2}D_{\mathrm{B}^{4+}}^0 - D_{\mathrm{Ti}}^0. \quad (2)$$

The site-averaged displacement magnitude change $\overline{\Delta D_A^0}$ and $\overline{\Delta D_B^0}$ gives the change in average site displacement (from $PbTiO_3$) due to alloying fraction x:

$$\overline{\Delta D_A^0} \equiv x\Delta D_A^0 = x(D_{\mathrm{Bi}}^0 - D_{\mathrm{Pb}}^0)$$
$$\overline{\Delta D_B^0} \equiv x\Delta D_B^0 = x\left(\frac{1}{2}D_{\mathrm{B}^{2+}}^0 + \frac{1}{2}D_{\mathrm{B}^{4+}}^0 - D_{\mathrm{Ti}}^0\right). \quad (3)$$

The D_M displacements in many alloys are well described as a linear function of $\overline{\Delta D_A^0}$ and $\overline{\Delta D_B^0}$. As an example, D_{Ti} data are fit in Fig. 2(a). We note that the data for $x = 0.25$ and $x = 0.50$ compositions fall into two distinct groups with similar slope b_{Ti}. The 0.5 $BiBO_3$ data in Fig. 2(a) are shifted upward from the 0.25 $BiBO_3$ data by a constant amount. This reflects the dependence of ΔD_{Ti} on $\bar{D}_A^0$, which is larger for $x = 0.5$ than for $x = 0.25$, due to the increase in Bi content. The change in the average cation displacement (ΔD_M) from its PT value due to substitution of x $BiB'_{1/2}B''_{1/2}O_3$ is modeled by

$$\Delta D_M = a_M\overline{\Delta D_A^0} + b_M\overline{\Delta D_B^0} = x(a_M\Delta D_A^0 + b_M\Delta D_B^0). \quad (4)$$

Quantifying the trends presented above, we fit Pb, Bi, Ti, Zr, Mg, and Zn displacements to Eq. (4) and plot the cation displacement D_M magnitudes from the model versus the actual DFT calculated values for all eight compositions studied [Fig. 2(b)]. The correlation is quite good, with all of the data points falling near the $y = x$ line. The a_M and b_M coupling constants are presented in Table III. All the cations, except Zn, are more sensitive to B-site changes than to A-site changes. The coupling constants for the x component of cation distortion are also larger than those for the total displacement.

The linear dependence of the cation displacement on $BiB'_{1/2}B''_{1/2}O_3$ fraction x gives rise to a quadratic dependence of P on x and nonmonotonic dependence of T_C on composition. The fraction of a given cation in solution is linear in x and each ion's displacement also exhibits a linear dependence on x [Eq. (4)]. The material polarization then has both linear and quadratic dependence on x.

$$P_{\mathrm{tot}} = \sum_M x_M(P_M^0 + Z_M^*\Delta D_M), \quad (5)$$

$$P_{\mathrm{tot}} = \sum_M [x_M P_M^0 + x_M^2 Z_M^*(a_M\Delta D_A^0 + b_M\Delta D_B^0)], \quad (6)$$

where P_M^0 is the polarization obtained by displacing ion M by its typical displacement (D_M^0) and Z_M^* is the Born effective charge. Since the Z^* tensors are isotropic for the cations, we omit the i and j subscripts. For the materials in our study, the use of displacement-independent Z^* is accurate (see supplementary material) and P_M^0 are just

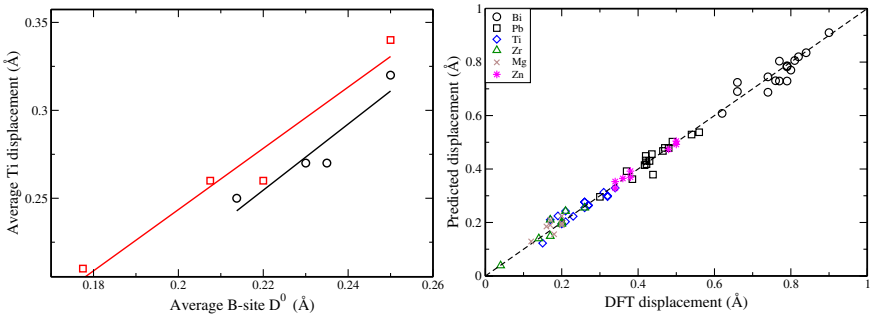

FIG. 2 (color online). (a) Total Ti displacement magnitude D_{Ti} versus the average B-site reference displacement value $\bar{D}_B^0$. Data for $x = 0.25$ $BiB'B''O^3$ and 0.50 $BiB'B''O^3$ compositions shown by circles and squares, respectively. (b) Correlation between average cation displacement magnitudes calculated by DFT and predicted from fits of DFT data to Eq. (4). Data for all eight compositions and for both x-component and total displacement magnitude are presented. The largest deviations from the line are observed for Bi data.

$Z^*_M D^0_M$. In cases where the dependence of Z^* on ionic displacement is important [32,33] P^0_M values can be obtained by integrating $Z^*(z)$ from 0 to D^0_M.

For the A site, the replacement of Pb ($D^0_{\mathrm{Pb}} = 0.45$ Å) by Bi ($D^0_{\mathrm{Bi}} = 0.8$ Å) increases the $\bar{D}^0_A$, promoting larger polarization. On the other hand, the large Ti displacement (0.28 Å) means that $BiB'_{1/2}B''_{1/2}O_3$ substitution into $PbTiO_3$ produces a negative ΔD^0_B, except in the case of BZT substitution. This gives rise to a negative quadratic dependence of P on x. The combination of a positive linear dependence on x and a negative quadratic dependence on x is the origin of the nonmonotonic changes in P and T_C.

The range of T_C behavior observed in $BiB'_{1/2}B''_{1/2}O_3$-PT solutions is due to the interplay between the linear and the quadratic terms in Eq. (6). In BZT-PT, the strong Zn off-centering does not inhibit A-site displacements ($\Delta D^0_B = 0$), leading to a steady increase in P and T_C. At the other extreme, in BMZ-PT the negative quadratic effect of A-B coupling is very strong ($\Delta D^0_B = -0.15$ Å) due to inclusion of Mg and Zr ions. This overpowers the favorable effect of greater Bi content and leads to a small initial decrease in P and T_C at $x = 0.25$ and then a much larger drop at $x = 0.5$.

The intermediate cases, BMT-PT and BZZ-PT solid solutions, show an initial rise in P due to the presence of Bi ions and moderate negative change in $\bar{D}^0_B$ ($\Delta D^0_B = -0.09$ Å for BMT and $\Delta D^0_B = -0.06$ Å for BMZ). However, as $BiB'_{1/2}B''_{1/2}O_3$ concentration is increased, the quadratic term dominates, leading to a turnover in P and T_C behavior with composition, and lower P and T_C values at $x = 0.50$.

In conclusion, we have shown that the nonmonotonic T_C trends in $BiBO_3$-PT solutions arise from the microscopic coupling between A-site and B-site displacements. The relationships between cation distortion and composition can be quantified in terms of average crystal chemical properties of the A and B sites, with the strongest effect given by compositional variation in the $\bar{D}^0_B$ parameter characterizing the off-centering ability of the B cation.

We thank P. K. Davies for discussions about crystal chemistry. This work was supported by the Office of Naval Research under Grant No. N-00014-00-1-0372. Computational support was provided by the Center for Piezoelectrics by Design, the DoD HPCMO, DURIP, and by the NSF CRIF program, Grant No. CHE-0131132.

[1] J. R. Cheng, R. E. Eitel, and L. E. Cross, J. Am. Ceram. Soc. **86**, 2111 (2003).
[2] L. Bellaiche, A. Garcia, and D. Vanderbilt, Phys. Rev. Lett. **84**, 5427 (2000).
[3] S. V. Halilov, M. Fornari, and D. J. Singh, Appl. Phys. Lett. **81**, 3443 (2002).
[4] I. Grinberg, V. R. Cooper, and A. M. Rappe, Nature (London) **419**, 909 (2002).
[5] P. Juhas and P. K. Davies, J. Am. Ceram. Soc. **87**, 2086 (2004).
[6] Y. Saito, H. Takao, T. Tani, T. Nonoyama, K. Takatori, T. Homma, T. Nagaya, and M. Nakamura, Nature (London) **432**, 84 (2004).
[7] D. I. Bilc and D. J. Singh, Phys. Rev. Lett. **96**, 147602 (2006).
[8] P. Baettig, C. F. Schelle, R. LeSar, U. V. Waghmare, and A. Spaldin, Chem. Mater. **17**, 1376 (2005).
[9] R. E. Eitel, C. A. Randall, T. R. Shrout, P. W. Rehrig, W. Hackenberger, and S.-E. Park, Jpn. J. Appl. Phys. **40**, 5999 (2001)
[10] J. I. Niguez, D. Vanderbilt, and L. Bellaiche, Phys. Rev. B **67**, 224107 (2003).
[11] M. R. Suchomel and P. K. Davies, J. Appl. Phys. **96**, 4405 (2004).
[12] M. R. Suchomel and P. K. Davies, Appl. Phys. Lett. **86**, 262905 (2005).
[13] R. Duan, R. F. Speyer, E. Alberta, and T. R. Shrout, J. Mater. Res. **19**, 2185 (2004).
[14] R. E. Eitel, S. J. Zhang, T. R. Shrout, C. A. Randall, and I. Levin, J. Appl. Phys. **96**, 2828 (2004).
[15] V. A. Isupov, Phys. Status Solidi A **181**, 211 (2000).
[16] V. A. Stephanovich, M. D. Glinchuk, and C. A. Randall, Phys. Rev. B **70**, 134101 (2004).
[17] N. J. Ramer and A. M. Rappe, Phys. Rev. B **59**, 12 471 (1999).
[18] A. M. Rappe, K. M. Rabe, E. Kaxiras, and J. D. Joannopoulos, Phys. Rev. B **41**, 1227 (1990).
[19] http://opium.sourceforge.net
[20] J. P. Perdew and A. Zunger, Phys. Rev. B **23**, 5048 (1981).
[21] P. Hohenberg and W. Kohn, Phys. Rev. **136**, B864 (1964).
[22] I. Grinberg and A. M. Rappe, Phys. Rev. B **70**, 220101(R) (2004).
[23] E. Cockayne and B. P. Burton, Phys. Rev. B **60**, R12542 (1999).
[24] I. Grinberg, V. R. Cooper, and A. M. Rappe, Phys. Rev. B **69**, 144118 (2004).
[25] I. Grinberg, M. R. Suchomel, W. Dmowski, P. K. Davies, and A. M. Rappe, Phys. Rev. Lett. (to be published).
[26] See EPAPS Document No. E-PRLTAO-98-006702 for more details of the Z^* polarization calculation methodology. For more information on EPAPS, see http://www.aip.org/pubservs/epaps.html.
[27] I. Grinberg, M. R. Suchomel, P. K. Davies, and A. M. Rappe, J. Appl. Phys. **98**, 094111 (2005).
[28] S. C. Abrahams, S. K. Kurtz, and P. B. Jamieson, Phys. Rev. **172**, 551 (1968).
[29] W. Zhong, R. D. King-Smith, and D. Vanderbilt, Phys. Rev. Lett. **72**, 3618 (1994).
[30] P. Ghosez, E. Cockayne, U. V. Waghmare, and K. M. Rabe, Phys. Rev. B **60**, 836 (1999).
[31] T. Egami, in *Fundamental Physics of Ferroelectrics: Proceedings of the Aspen Center for Physics Winter Workshop*, edited by R. E. Cohen (American Institute of Physics, Melville, New York, 2000), pp. 16–25.
[32] P. Ghosez, J.-P. Michenaud, and X. Gonze, Phys. Rev. B **58**, 6224 (1998).
[33] J. B. Neaton, C. Ederer, U. V. Waghmare, N. A. Spaldin, and K. M. Rabe, Phys. Rev. B **71**, 014113 (2005).